Modeling and Simulation of Shell and Tube Heat Exchangers under Milk Fouling

Michael C. Georgiadis, Guillermo E. Rotstein, and Sandro Macchietto
Centre for Process Systems Engineering, Imperial College of Science, Technology and Medicine, London SW7 2BY, U.K.

A mathematical model for single shell and tube heat exchangers under milk fouling is presented. A fouling model based on a reaction/mass-transfer scheme is detailed in which the main factors during milk heat treatment are quantified in a formal way. This model is coupled with a detailed dynamic model of a shell-and-tube heat exchanger where both radial and axial domains are taken into account. An analytical procedure for the calculation of key parameters provides the means to achieve more accuracy. The simulation results agree well with available experimental work. Four different heat-exchanger arrangements are then considered to illustrate their impact on the fouling behavior. The results are encouraging enough to validate current operating industrial techniques for fouling mitigation. For a given thermal duty, short heat exchangers are more prone to fouling due to high-temperature requirements and milk should be heated as gradually as possible to minimize fouling. The results show that there are main tradeoffs between design and operation issues.

Introduction

A variety of heat treatments is employed in the food industries. A typical and important example is dairy pasteurization where, when milk is heated and as the result of its instability, a deposit of milk solids is formed in the heat-exchanger surface. Although this deposit is not sufficient to affect milk composition significantly, it results in hydraulic and thermal disturbances and creates the need for cleaning operations which have to be carried out to bring the exchanger surface back to its original state. Fouling in dairy plants is a severe problem compared with other industries. For example, while in the petrochemical refineries, heat exchangers may only be cleaned annually, in the dairy industry it is common practice to clean them every 5–10 h. It should be noted here that the operating cost of fouling in the U.S. fluid milk industry (pasteurized milk production, that is, no sterilized and ultrahigh temperature milk) has been estimated in \$140 millions per year, approximately at current prices (Sandu and Singh, 1991).

Milk fouling has been studied for a number of years. The composition of the deposit is known and the chemical changes that occur when heating milk are fairly well understood. There are two key contributions in this area: the work of Fryer et al. (1996) and the work at the food technology and food process engineering laboratory in France (Lalande et al., 1989).

The key role played by proteins and especially β-lactoglobulin has been recognized in most recent milk fouling studies. Lalande et al. (1985) were the first who investigated the effect of β-lactoglobulin denaturation in milk fouling and showed that heat denaturation of this protein governs the milk deposit formation on the heat-transfer area. De Jong et al. (1992) applied the kinetics of the β-lactoglobulin reaction to analyze fouling in plate heat exchangers, and found that the amount of deposit could be correlated with protein reaction rates.

An interesting analysis concerning the chemical reactions governing fouling is presented by Paterson and Fryer (1988). They proved, following some principles of reaction engineering, that milk fouling is generated by chemical reaction(s) and the reaction(s) occur throughout the region of the fluid which is hot enough to support significant reaction rates. This means that there is no reason to assume that the rate controlling step in reaction fouling is the surface reaction. It also implies that bulk reactions could be significant together with mass transfer from the bulk region to the hot sublayer. Building

Correspondence concerning this article should be addressed to S. Macchietto.

upon this analysis, Belmar-Beiny et al. (1993) studied the effect of Reynolds Numbers and fluid temperature in whey protein fouling. They showed that fouling is significantly increased as the fluid is heating up. Two possible mechanisms were considered: (i) Fouling is mass-transfer controlled and (ii) fouling is reaction controlled. Later, Toyoda and Fryer (1997) presented a very detailed fouling model which takes account of mass transfer between bulk and layer. Recently, Fryer et al. (1996) developed a statistical model for fouling of a plate heat exchanger. Based on a statistically-designed series of experiments, they studied and quantified the significance of a number of factors, including β-lactoglobulin reaction rate, on fouling within an ultrahigh temperature process.

Delplace et al. (1994) studied fouling in plate heat exchangers (PHE) using whey proteins solutions. Using a temperature profile determined numerically, the quantity of β-lactoglobulin denaturated during heat treatment was calculated. Delplace and Leuliet (1995) also studied fouling of a PHE with different flow arrangements. An empirical model was developed in order to predict the dry mass of deposit in the PHEs channels based on the heat denaturation of β-lactoglobulin.

Sandu (1989) presents a considerable amount of work on milk fouling in plate heat exchangers. He developed a detailed physicomathematical model where fouling kinetics and dynamics were defined based on experimental results. Sandu and Lund (1982) developed a general model for fouling dynamics for the simple case of an inverse-solubility salt under the assumption that the deposition rate is entirely mass-transfer controlled. This model was extended under more assumptions for fluids, which are multicomponent systems. No simulation results were presented.

So far, in most cases, fouling has been modeled with a simple representation of the hydrodynamics of heat exchanger. However, it is known that there are strong interactions between the physicochemical, hydro- and thermodynamic fundamentals involved in fouling. For example, if mass-transfer operations are important these are determined by the boundary layer thickness which depends on the fluid velocity. It is, therefore, important to consider all the relevant transport phenomena which take place during milk heat treatment together with the fouling kinetics.

Accurate prediction and analysis of fouling dynamics for a given system would pave the way for obtaining the optimal design and operating policies for industrial heat exchangers. The need for optimizing dairy plants suffering severe fouling problems has been long recognized (Fryer, 1989; Sandu and Lund, 1983). It is clear that the use of realistic and detailed models to optimize the equipment design and control can result in substantial economic benefits.

In this article we use fundamental kinetic theories to perform a comprehensive study of milk fouling as a process affected by momentum, heat- and mass-transfer phenomena. For this purpose, a fouling model taken from Toyoda and Fryer (1997) is coupled together with a detailed dynamic heat-exchanger model, where transport phenomena are taken into account in detail. Four different types of heat exchangers are considered to illustrate how the fouling behavior is affected. The simulation results are encouraging. They are verified against available experimental data and current industrial techniques for fouling mitigation.

The mathematical model is presented which is used to describe the behavior of shell- and tube-heat exchangers under milk fouling. In the section on numerical simulation and results, the simulation results are presented for the four cases of operation together with verification.

Mathematical Model

Fouling model

A fouling model must take into account all the relevant factors during milk heat treatment such as fluid velocity, milk composition, and temperature. It is generally agreed now that fouling is controlled by reactions, but it is still not clear if these are bulk or layer reactions or a combination of both. Mass transfer between the bulk and layer may be also important. Here the β-lactoglobulin reaction scheme is used for the fouling model. When milk is heated above 65°C, β-lactoglobulin becomes thermally unstable and it unfolds in molecular *denaturation* exposing reactive sulphydry ($-$SH) groups and polymerizes irreversibly to give insoluble particles in *aggregation* (De Jong et al., 1992). The key step in studying fouling is to capture the interrelationship between the chemical reactions which give rise to deposition and the fluid mechanics associated with the heat-transfer equipment.

The reaction/mass-transfer scheme is shown in Figure 1 and is the most detailed in the literature. It was adopted from Toyoda and Fryer (1997) and was first proposed by De Jong et al. (1992). The reaction scheme is described as follows:

- Proteins react in both the bulk and the thermal boundary layer in the milk. Native protein N is transformed to denaturated protein D in a first-order reaction. The denaturated protein then reacts to give aggregated protein A in a second-order reaction.
- Mass transfer between the bulk and the thermal boundary layer takes place for each protein.
- Only the aggregated protein is deposited on the wall. The deposition rate is proportional to the concentration of aggregated protein in the thermal boundary layer.
- The fouling resistance to heat transfer is proportional to the thickness of the deposit.

The reaction rate constants are expressed in the common form as

$$k = k_o \exp\left(\frac{-E}{RT}\right)$$

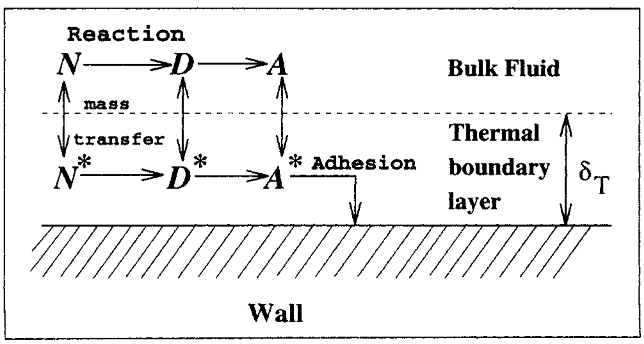

Figure 1. Protein reaction scheme used in the fouling model.

Table 1. Kinetic Data for the Reactions of β-Lactoglobulin

k_{No} kJ/mol	k_{Do} kJ/mol	E_N 1/s	E_D $m^3/(kg \cdot s)$	Temp. °C
261	312	3.37×10^{37}	1.36×10^{43}	70–90
—	—	56	1.83×10^{6}	90–150

The pre-exponential factors k_o and the activation energies for the two reactions are taken from De Jong et al. (1992) and given in Table 1 where the subscripts N and D refer to the first and second reaction, respectively.

Shell-and-tube heat-exchanger model under fouling

In previous work on heat exchangers under fouling very simple models were used to account for the hydro- and thermodynamic characteristics of the fluid. Two common assumptions were:

- The fluid temperature in the bulk and thermal boundary layer are radially uniform, that is, the temperature in the bulk and thermal boundary layer are equal and do not change with the tube radius.
- The fluid flows in plug flow at uniform velocity. The velocity in the thermal boundary layer is assumed negligible in comparison.

The above assumptions simplify the conservation laws expressed by partial differential equations describing the hydrodynamics, the reactions, and mass transfer between the bulk and the layer. However, under turbulent flow conditions, velocity is not uniform and a profile exists (Brodkey and Hershey, 1988).

It is then apparent that the physical behavior may change significantly in the radial direction. The radial velocity profile may affect considerably both the heat- and the mass-transfer operations. Furthermore, a radial temperature profile in the bulk exists which also affects the rate of the reactions and mass transfer. If these profiles are ignored, potential differences between bulk and boundary reaction rates are not captured. Note that milk fouling is determined by reactions rates, which are strong functions of temperature.

Here, we present a detailed model for shell-and-tube heat exchangers under fouling by relaxing the above assumptions and taking into account the radial dependency of velocity, temperature, and concentrations. In order to be consistent with the proposed reaction scheme, where mass-transfer operations occur between the bulk and the thermal boundary layer, we distinguish the bulk from the layer on the conservation laws. The velocity in the thermal boundary layer, which is small but not negligible, is taken into account.

The following are typical assumptions which are considered for the purpose of modeling:

- The variation of the physical properties of milk with temperature was neglected, and the properties were taken as those of skimmed milk (McKetta, 1984). However, transport properties are calculated in detail.

Table 2. Values of Particle Diameters for the Three Proteins

Particles		
Native	Denaturated	Aggregated
7.5×10^{-11} m	7.5×10^{-11} m	4.2×10^{-10} m

Table 3. Details of Heat Exchangers Used in Simulation (Steady State)

Case of Oper.	Type of Exchanger	Length m	T_f^{in} K	T_f^{out} K	T_s^{in} K	T_s^{out} K
1	Steam, $T_w = 374$ K	10	333	370.4	—	—
2	Steam, $T_w = 390$ K	5	333	370.4	—	—
3	Hot water, cocurrent flow	10	333	370.4	385	374
4	Hot water, countercurrent flow	7	333	370.4	385	374

- The overall heat-transfer resistance is determined by that on the tube side fluid (milk).
- The concentration and temperature for proteins at the boundary layer are assumed not to be radially dependent.

In the operating scenario considered, a stream of skimmed milk (0.25 kg/s) is to be heated from 333 K to a target temperature of approximately 370 K. Tables 3 and 4 give the specification of the heat exchangers prior to the initiation of the fouling. Four cases were examined (Figure 2): (a) The heating medium is steam at temperature 374 K. (b) The heating medium is steam at temperature 390 K. (c) The heating medium is hot water at 385 K in co-current flow with milk. (d) The same as in case (c) but in a countercurrent operation. Similar data for the steady-state milk inlet and outlet temperatures were used by Fryer and Slater (1985) and approximately correspond to industrial conditions.

Fundamental equations

Consider a differential element in a circular tube, where r_o is the inner radius, and L is the length of the tube (Figure 3). Then material balances of proteins in the bulk are given by the following equations

Native Protein

$$\frac{\partial C_N}{\partial t} + u_z(r)\frac{\partial C_N}{\partial z} = -k_{No}\exp\left(\frac{-E_N}{RT_f(r)}\right)\cdot C_N + \frac{1}{r}\frac{\partial}{\partial r}\left(r\cdot D_N\frac{\partial C_N}{\partial r}\right) + \frac{\partial}{\partial z}\left(D_N\frac{\partial C_N}{\partial z}\right) \quad (1)$$

Denaturated Protein

$$\frac{\partial C_D}{\partial t} + u_z(r)\frac{\partial C_D}{\partial z} = k_{No}\exp\left(\frac{-E_N}{RT_f(r)}\right)\cdot C_N - k_{Do}\exp\left(\frac{-E_D}{RT_f(r)}\right)\cdot C_D^2 + \frac{1}{r}\frac{\partial}{\partial r}\left(r\cdot D_D\frac{\partial C_D}{\partial r}\right) + \frac{\partial}{\partial z}\left(D_D\frac{\partial C_D}{\partial z}\right) \quad (2)$$

Table 4. Heat-Exchanger Data Used in Simulation

Milk Flow Rate, kg/s	Hot Water Flow Rate, kg/s	Diameter m	α_s 1/m	v_s m/s
0.25	1.5	0.025	160	4.08

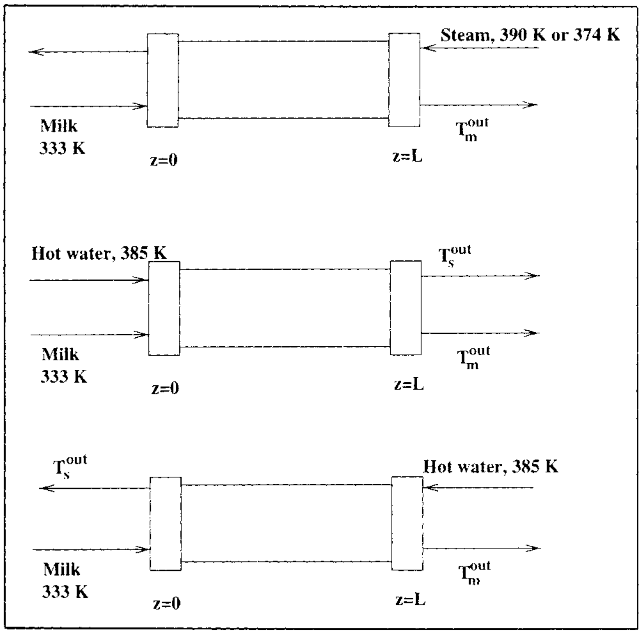

Figure 2. Shell-and-tube heat exchangers for milk heat treatment.

Aggregated Protein

$$\frac{\partial C_A}{\partial t} + u_z(r)\frac{\partial C_A}{\partial z} = k_{Do}\exp\left(\frac{-E_D}{RT_f(r)}\right)\cdot C_D^2 + \frac{1}{r}\frac{\partial}{\partial r}\left(r\cdot D_A\frac{\partial C_A}{\partial r}\right) + \frac{\partial}{\partial z}\left(D_A\frac{\partial C_A}{\partial z}\right) \quad (3)$$

The last two righthand side terms express the rate of diffusion into the control volume with respect to the radial and axial distance. In the above equations, $u_z(r)$ is the fluid velocity as a function of the tube radius and D_N, D_D, D_A are the diffusion coefficients of the three proteins.

For the proteins at the layer, radial gradients of the concentrations are not considered but terms are included to account for radial mass transfer via mass-transfer coefficients.

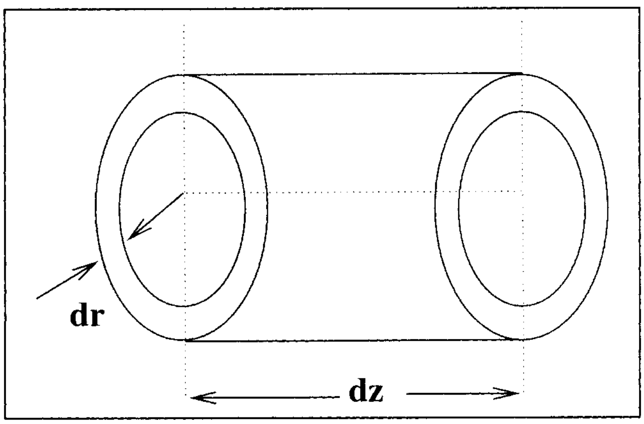

Figure 3. Differential element in a shell-and-tube heat exchanger.

In order to distinguish between bulk and surface reactions rates, the last are assumed to take place at the interface temperature T_i which is radially independent. The assumption of constant T_i provides an approximate way to distinguish bulk and surface reaction rates. On the other hand, diffusion in the axial direction is considered. Thus, the material balances of the proteins in the thermal boundary layer are given by

Native Protein

$$\frac{\partial C_N^*}{\partial t} + u_z(r)\frac{\partial C_N^*}{\partial z} = -k_{No}\exp\left(\frac{-E_N}{RT_i}\right)\cdot C_N^* - \frac{k_{mN}}{\delta_T}(C_N^* - C_N) + \frac{\partial}{\partial z}\left(D_N\frac{\partial C_N^*}{\partial z}\right) \quad (4)$$

Denaturated Protein

$$\frac{\partial C_D^*}{\partial t} + u_z(r)\frac{\partial C_D^*}{\partial z} = k_{No}\exp\left(\frac{-E_N}{RT_i}\right)\cdot C_N^* - k_{Do}\exp\left(\frac{-E_D}{RT_i}\right)\cdot C_D^{*2} - \frac{k_{mD}}{\delta_T}(C_D^* - C_D) + \frac{\partial}{\partial z}\left(D_D\frac{\partial C_D^*}{\partial z}\right) \quad (5)$$

Aggregated Protein

$$\frac{\partial C_A^*}{\partial t} + u_z(r)\frac{\partial C_A^*}{\partial z} = k_{Do}\exp\left(\frac{-E_D}{RT_i}\right)\cdot C_D^{*2} - \frac{1}{\delta_T}\cdot[k_{mA}(C_A^* - C_A) + k_w C_A^*] + \frac{\partial}{\partial z}\left(D_A\frac{\partial C_A^*}{\partial z}\right) \quad (6)$$

where C_N, C_D and C_A are the values of the bulk protein (kg/m^3) in contact with the boundary layer and δ_T is the thickness of the thermal layer. Finally, k_{mN}, k_{mD}, k_{mA} are the protein mass-transfer coefficients.

The rate of deposition is related to the concentration of aggregated protein in the layer by the mass-transfer coefficient k_w. The dimensionless Biot number is used to express the change of heat transfer due to fouling, and it is related to the rate of deposition by a constant β (Toyoda and Fryer, 1997; Fryer and Slater, 1985)

$$\frac{\partial Bi}{\partial t} = \beta k_w C_A^* \quad (7)$$

The energy balance on the milk side can be written as

$$\rho C_p\frac{\partial T_f(r)}{\partial t} + \rho C_p\cdot u_z(r)\frac{\partial T_f(r)}{\partial z} = \frac{\partial}{\partial z}\left(k_f\frac{\partial T_f(r)}{\partial z}\right) + \frac{1}{r}\frac{\partial}{\partial r}\left(rk_f\frac{\partial T_f(r)}{\partial r}\right) \quad (8)$$

Here, hot water is adopted as the heating medium for the countercurrent and cocurrent operation. It is assumed that its temperature and velocity are radially uniform. Under this assumption, the energy balance for the heating medium takes the following form

- Cocurrent operation with milk

$$\frac{\partial T_s}{\partial t} + v_s \frac{\partial T_s}{\partial z} = -\frac{1}{\rho_w C_{pw}} \cdot U \cdot \alpha_s (T_s - T_f) \quad (9)$$

- Countercurrent operation with milk

$$\frac{\partial T_s}{\partial t} - v_s \frac{\partial T_s}{\partial z} = -\frac{1}{\rho_w C_{pw}} \cdot U \cdot \alpha_s (T_s - T_f) \quad (10)$$

where u_s is the heating medium velocity (m/s) and α_s is the shell heat-transfer area per unit volume and can be taken equal to $4/d$ where d is the tube diameter.

Another alternative explored was the use of steam as heating medium. In this case it is assumed that steam enters and exits the exchanger at the same temperature (that is, flow rate is high enough for the given thermal duty) providing its heat of condensation for the heating purposes.

Boundary conditions

Proteins in the Bulk. The integration in the radial direction should be carried out from $r = 0$ (center of the tube) to $r = r_o - \delta_T$ where δ_T is the thermal boundary layer (see Figure 1). However, the thickness of the boundary layer is very small compared with the tube radius and a typical value for the constant wall temperature operation is 0.023 mm. It is then reasonable to assume that the mass balance equations are integrated over the entire range of the tube radius.

Danckwerts (1953) boundary conditions are utilized at the inlet and outlet of the tube

$$-D_N \cdot \frac{\partial C_N}{\partial z} = u_z(r)(C_{N,\text{in}} - C_N) \quad z = 0, r \in [0, r_o] \quad (11)$$

$$-D_A \cdot \frac{\partial C_A}{\partial z} = u_z(r)(C_{A,\text{in}} - C_A) \quad z = 0, r \in [0, r_o] \quad (12)$$

$$-D_D \cdot \frac{\partial C_D}{\partial z} = u_z(r)(C_{D,\text{in}} - C_D) \quad z = 0, r \in [0, r_o] \quad (13)$$

$$\frac{\partial C_N}{\partial z} = 0.0 \quad z = L, r \in [0, r_o] \quad (14)$$

$$\frac{\partial C_D}{\partial z} = 0.0 \quad z = L, r \in [0, r_o] \quad (15)$$

$$\frac{\partial C_A}{\partial z} = 0.0 \quad z = L, r \in [0, r_o] \quad (16)$$

while the inlet protein concentrations take the following values

$$C_{N,\text{in}} = 3.8 \text{ kg/m}^3 \quad (17)$$

$$C_{D,\text{in}} = 0.0 \text{ kg/m}^3 \quad (18)$$

$$C_{A,\text{in}} = 0.0 \text{ kg/m}^3 \quad (19)$$

The above is a typical value for the inlet native concentration, while the concentration of denaturated protein may sometimes be above zero due to a heat pre-treatment of milk (McKetta, 1984).

The main transfer rate balance at the interface between the bulk and the layer yields

$$-D_N \frac{\partial C_N}{\partial r} = k_{mN}(C_N - C_N^*) \quad r = r_o, z \in (0, L) \quad (20)$$

$$-D_D \frac{\partial C_D}{\partial r} = k_{mD}(C_D - C_D^*) \quad r = r_o, z \in (0, L) \quad (21)$$

$$-D_A \frac{\partial C_A}{\partial r} = k_{mA}(C_A - C_A^*) \quad r = r_o, z \in (0, L) \quad (22)$$

while radial symmetry dictates that

$$\frac{\partial C_N}{\partial r} = 0.0 \quad r = 0, z \in (0, L) \quad (24)$$

$$\frac{\partial C_D}{\partial r} = 0.0 \quad r = 0, z \in (0, L) \quad (25)$$

$$\frac{\partial C_A}{\partial r} = 0.0, \quad r = 0, z \in (0, L) \quad (26)$$

Layer Proteins

$$-D_N \cdot \frac{\partial C_N^*}{\partial z} = u_z(r)(C_{N^*,\text{in}} - C_N^*) \quad z = 0 \quad (27)$$

$$-D_D \cdot \frac{\partial C_D^*}{\partial z} = u_z(r)(C_{D^*,\text{in}} - C_D^*) \quad z = 0 \quad (28)$$

$$-D_A \cdot \frac{\partial C_A^*}{\partial z} = u_z(r)(C_{A^*,\text{in}} - C_A^*) \quad z = 0 \quad (29)$$

$$\frac{\partial C_N^*}{\partial z} = 0.0 \quad z = L \quad (30)$$

$$\frac{\partial C_D^*}{\partial z} = 0.0 \quad z = L \quad (31)$$

$$\frac{\partial C_A^*}{\partial z} = 0.0 \quad z = L \quad (32)$$

where the inlet ($z = 0$) concentrations of the layer proteins are the following

$$C_{N^*,\text{in}} = 3.8 \text{ kg/m}^3 \quad (33)$$

$$C_{D^*,\text{in}} = 0.0 \text{ kg/m}^3 \quad (34)$$

$$C_{A^*,\text{in}} = 0.0 \text{ kg/m}^3 \quad (35)$$

Energy Balance. The boundary conditions for all the heat-exchanger arrangements considered are as follows

$$-k_f \frac{\partial T_f(r)}{\partial z} = \rho C_p u_z(r)\left[T_f^{\text{in}} - T_f(r)\right] \quad z = 0, r \in [0, r_o] \quad (36)$$

$$\frac{\partial T_f(r)}{\partial z}=0 \qquad z=L,\ r\in[0,r_o] \tag{37}$$

$$\frac{\partial T_f(r)}{\partial r}=0 \qquad r=0,\ z\in(0,L) \tag{38}$$

$$k_f\cdot\frac{\partial T_f(r)}{\partial r}=U\cdot[T_w-T_f(r)] \qquad r=r_o,\ z\in(0,L) \tag{39}$$

$$k_f\cdot\frac{\partial T_f(r)}{\partial r}=U\cdot[T_s(z)-T_f(r)] \qquad r=r_o,\ z\in(0,L) \tag{40}$$

Equation 39 is for the constant wall temperature case only (that is, steam as the heating medium), while Eq. 40 is for the countercurrent (or cocurrent) case. U is the overall heat-transfer coefficient, which is a function of the fouling resistance (Biot number), and T_f^{in} is the milk inlet temperature equal to 333 K. Finally, T_w and $T_s(z)$ are the wall and the heating medium temperature (K), respectively.

The boundary conditions for the heating medium are given below

$$\text{Cocurrent operation} \quad T_s(z)=385\text{ K} \quad z=0 \tag{41}$$

$$\text{Countercurrent operation} \quad T_s(z)=385\text{ K} \quad z=L \tag{42}$$

Initial conditions

It is assumed that prior to the circulation of milk (such as initiation of fouling) the exchanger was operating at steady state with a nonfouling fluid on the tube site. This is justified since pasteurizers are preheated and sterilized with hot water before the milk fluid is processed

$$\frac{\partial T_f(z,r,t)}{\partial t}=0 \quad t=0,\ \forall z\in(0,L) \quad \forall r\in(0,r_o) \tag{43}$$

$$\frac{\partial T_s(z,t)}{\partial t}=0 \quad t=0,\ \forall z\in(0,L) \tag{44}$$

$$C_N(z,r,t)=C_D(z,r,t)=C_A(z,r,t)=0.0 \qquad t=0,\ \forall z\in(0,L) \quad \forall r\in(0,r_o) \tag{45}$$

$$C_N^*(z,t)=C_D^*(z,t)=C_A^*(z,t)=0.0 \qquad t=0,\ \forall z\in(0,L) \tag{46}$$

$$Bi(z,t)=0.0 \quad t=0,\ \forall z\in(0,L) \tag{47}$$

Calculation of transport phenomena variables

The model of a shell-and-tube heat exchanger under fouling includes a number of variables such as the thickness of the thermal boundary layer δ_T, the mass-transfer coefficients k_{mN}, k_{mD}, k_{mA}, k_w, and the fluid velocity $u_z(r)$. Here, detailed expressions are used for the calculation of these variables.

The thickness of the thermal boundary layer δ_T is to that of the laminar boundary layer δ using the following expressions

$$\frac{\delta_T}{\delta}=Pr^{1/3} \tag{48}$$

where Pr is the Prandtl number given by

$$Pr=\frac{C_p\cdot\mu}{k_f} \tag{49}$$

The above two expressions illustrate the analogy between the momentum and heat transfer in turbulent flow conditions (Brodkey and Hershey, 1988). In order to calculate δ, one can assume that it is equal to the thickness of the viscous sublayer. It is known that during milk heat treatment the flow is turbulent (that is, Reynolds number greater than 2,100). Therefore, the velocity profiles within the flow can now be expressed as (Brodkey and Hershey, 1988)

$$\text{Viscous sublayer:} \quad u^+=y^+ \text{ for } 0<y^+\le 5 \tag{50}$$

$$\text{Generation zone:} \quad u^+=5\ln y^+-3.05 \text{ for } 5<y^+<30 \tag{51}$$

$$\text{Turbulent core:} \quad u^+=2.5\ln y^+ +5.5 \text{ for } 30\le y^+ \tag{52}$$

where u^+ is a dimensionless velocity and y^+ the dimensionless distance from the wall defined as

$$u^+=\frac{u_z(r)}{U^*},\qquad y^+=\frac{y\cdot U^*\cdot\rho}{\mu} \tag{53}$$

where U^* is the friction velocity, is a function of the wall shear stress τ_w and is given by the following equations

$$U^*=\sqrt{\left(\frac{\tau_w}{\rho}\right)} \tag{54}$$

It is now possible using Eqs. 50 and 53 to calculate δ for y^+ equal to 5 (by setting δ equal to y since it is equal to the thickness of the boundary layer).

The wall shear stress τ_w can be calculated using the following expressions which hold for the case of turbulent flow

$$f=0.079\,N_{Re}^{1/4} \tag{55}$$

$$f=\frac{\tau_w}{\frac{1}{2}\rho u_{z,\text{aver}}^2} \tag{56}$$

$$Re=\frac{d\cdot u_{z,\text{aver}}\cdot\rho}{\mu} \tag{57}$$

where f is the friction factor and $u_{z,\text{aver}}$ is the average velocity which can easily be calculated from the fluid flow rate w_f as follows

$$u_{z,\text{aver}}=\frac{w_f}{\rho\cdot\text{Area}} \qquad \text{Area}=\frac{\pi\cdot d^2}{4} \tag{58}$$

Finally, the mass-transfer coefficients for the three proteins are related to the diffusion coefficients by

$$\dot{k}_L = \frac{D_F}{\delta} \tag{59}$$

When the diameter of the particles is known, the diffusion coefficients can be estimated by the Wilke-Chang equation (Perry and Green, 1984)

$$D_F = 1.310^{-17} \frac{T_i}{\mu V_F^{0.6}} \tag{60}$$

with V_F as the molecular volume of the absorbed particles

$$V_F = N_{AV} \frac{1}{6} \pi d_F^3 \tag{61}$$

where N_{AV} is the Avogadro constant $6.023 \cdot 10^{23}$, and d_F is the particle diameter which must be determined experimentally. Unfortunately, their values for milk are not reported in the literature. De Jong et al. (1992) performed a regression analysis with several supposed particle diameters, and they concluded that the highest correlation coefficients were obtained with particle diameters smaller than 10 nm and very close to 10^{-10} m; mean diameters above 50 nm did not give satisfactory agreement with the experimental results. Here, the values of the particles diameters are estimated using optimal regression methods in order to achieve a good agreement with experimental work, while taking into account the size limitations reported by the above researchers (Table 2). This is discussed in more detail in the subsection on parameter estimation.

A key assumption made in the calculation of the transport properties is that the turbulent contribution as expressed by the eddy diffusivity of mass and heat transfer is neglected. For the transport properties in the layer, the turbulent contribution is small ($\sim 10^{-8}$) compared with the values of the Fickian diffusivities ($\sim 10^{-6}$). On the other hand, for the bulk this contribution may be considerable. A sensitivity analysis has been performed using approximate values for the eddy diffusivities in the bulk. The analysis indicates that there is a less than 2% change in the simulation results which can be considered as acceptable within the experimental error.

The value of the mass-transfer coefficient to the deposit k_w is given by Toyoda and Fryer (1997) and it is equal to 10^{-7} m/s. Finally, the proportionality constant β can be determined only by experimental data. Here, a value of 58 m^2/kg was obtained from the parameter estimation problem (see the section on parameter estimation).

Radial Velocity Profile. Although Eqs. 50 to 52 provide a good description of the velocity distribution for flow in the tubes, they introduce discontinuities in the model which may cause numerical difficulties in the simulation. Alternatively, it is possible to use the Pai's continuous model for the radial velocity distribution, under turbulent flow conditions, described by the following equations (Brodkey and Hershey, 1988)

$$\frac{u_z(r)}{u_{z,\max}} = 1 + \alpha_1 \left(\frac{r}{r_o} \right)^2 + \alpha_2 \left(\frac{r}{r_o} \right)^{2m} \tag{62}$$

where the terms α_1 and α_2 are given as follows:

$$\alpha_1 = \frac{(s-m)}{(m-1)} \tag{63}$$

$$\alpha_2 = \frac{(1-s)}{(m-1)} \tag{64}$$

and m can be expressed as the whole integer closest up or down to the value given by

$$m = -0.617 + (8.211 \times 10^{-3})(N_{Re})^{0.786} \tag{65}$$

Finally, the quantity s can be correlated in terms of the Reynolds number N_{Re}

$$s = 0.585 + (3.172 \times 10^{-3})(N_{Re})^{0.833} \qquad 2{,}800 < N_{Re} \tag{66}$$

Note that the maximum velocity $u_{z,\max}$ is a function of the average velocity

$$\frac{u_{z,\max}}{u_{z,\text{aver}}} = 1 + \frac{\alpha_1}{2} + \frac{\alpha_2}{(m+1)} \tag{67}$$

The above model equations provide a continuous model of the velocity radial profile which is quite accurate for Reynolds number less than 100,000 (Brodkey and Hershey, 1988). Since, due to pressure drop limitations, it is not possible to exceed this value for the problem considered here, these equations were adopted for the simulation results presented in the next section.

Quantifying fouling

Additional variables allow us to quantify fouling. Since the Biot number is a function of the tube distance z (it is determined by the aggregated protein concentration), an average Biot number can be defined over the heat exchanger as

$$\overline{Bi} = \frac{1}{L} \int_o^L Bi(z)\,dz \tag{68}$$

The thickness (m) of the deposit x_d at each position z along the heat exchanger can be defined using the Biot number as

$$x_d(z) = \frac{\lambda_d \cdot Bi(z)}{U_o} \tag{69}$$

where λ_d is the deposit thermal conductivity equal to 0.5 W/m·K (LeClercq-Perlat and Lalande, 1991) and the overall heat-transfer coefficient under clean conditions U_o can be easily determined for a given thermal duty and heat-transfer area.

An average deposit thickness is defined over the tube by the following equation

$$\bar{x}_d = \frac{1}{L} \int_o^L x_d(z)\,dz \tag{70}$$

The deposit mass at each position z along heat exchanger, expressed in kg/m^2 is defined as

$$\text{mass}(z) = \frac{\lambda_d \cdot Bi(z) \cdot \rho_d}{U_o} \tag{71}$$

where ρ_d is the deposit density 1,030 kg/m^3.

Similarly, the average deposit mass over the tube is

$$\overline{\text{mass}} = \frac{1}{L}\int_o^L \text{mass}(z)dz \tag{72}$$

Another way to quantify fouling is by the "fictitious" efficiency of the heat exchanger given by the following equation

$$\epsilon_{fic} = \frac{\text{Heat exchanged during operation without control}}{\text{maximal heat exchanged}} = \tag{73}$$

$$\frac{T_f^{\text{outlet}}(t) - T_f^{\text{in}}}{T_f^{\text{out}}(0) - T_f^{\text{in}}} \quad \forall t \in (0, \tau] \tag{74}$$

where $T_f^{\text{out}}(0)$ is the milk outlet temperature (K) at steady state (before fouling), which is specified to be 370.4 K, $T_f^{\text{outlet}}(t)$ is the same temperature during the heating operation and τ is the total heating period.

The overall heat-transfer coefficient U (W/m$^2 \cdot$k) and the interface temperature T_i are given by the following expressions (Fryer and Slater, 1985)

$$U = \frac{U_o}{1+Bi} \tag{75}$$

$$T_i = \frac{T_w + BiT_f}{1+Bi} \quad \text{steam as heating fluid} \tag{76}$$

$$T_i = \frac{T_s + BiT_f}{1+Bi} \quad \text{hot water as heating fluid} \tag{77}$$

Numerical Simulation and Results

The model of a shell-and-tube heat exchanger under milk fouling described by Eqs. 1 to 77 comprises a set of integral, partial differential, and algebraic equations (IPDAEs). It is simulated using the simulation package gPROMS (Oh and Pantelides, 1996; Barton and Pantelides, 1994). The solution method is based on a two-phase method-of-lines approach (see Figure 4). In the first phase, the spatial dimensions (axial and radial) are discretized in terms of finite dimensional representations and this reduces the IPDAEs into sets of differential algebraic equations (DAEs) with respect to time. In the second phase, the DAEs are integrated over the time horizon of interest using appropriate integration techniques. Here, the axial domain is discretized using second-order orthogonal collocation on 20 uniform finite elements, whereas the radial domain is approximated by third-order orthogonal collocation of five finite elements. This number of elements and order of approximation over the two spatial domains provides the most accurate results. A number of simulations

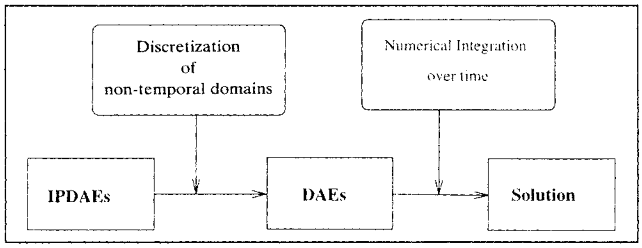

Figure 4. Solution strategy of the model.

tests have been performed, which indicated that if less than 12 elements are to be used for the axial domain discretization there is a 5–10% change in the results. On the other hand, the discretization over the radial domain is sensitive if less than three elements and/or a second-order approximation is used. The data used in simulation are given in Tables 1 to 4.

Parameter estimation and verification: simulation vs. experimental data

There are a few publications in the literature where experimental results of milk fouling in a tube are reported. Verification of the simulation results is an important step in order to:

- Check the validity of the model presented here.
- Determine appropriate values for certain parameters (such as particle diameters)

There are four unknown parameters in the model presented in the Mathematical Model section. These are the diameters of the three protein particles and the deposition rate constant β. Only size limitations for the particles are reported in the literature (see the section on Calculation of the Transport Phenomena Variables). Taking into account these limitations, a parameter estimation analysis is performed based on the solution of a dynamic optimization problem. This problem was solved in order to take into account the constraints in the particles diameters. It should be emphasized here that the mass-transfer coefficient is taken as constant (from Toyoda and Fryer, 1997) since there are no data concerning even approximate order of its magnitude. Therefore, any attempt to find its optimal value may lead to unrealistic values. A brief description of the mathematical problem being solved is given in the Appendix. The optimal values of the particle diameters are given in Table 2, while the constant β was found to be 58. It is worthwhile to notice that the obtained values are very close to the conclusions of De Jong et al. (1992).

Here, for the purpose of parameters estimation and verification, we use the experimental results of Belmar-Beiny et al. (1993). The experimental conditions are: 1% whey protein; Reynolds number 6,250; heating period 1 h, length of the tube 1.5 m and two sets of fluid inlet and outlet temperature, as indicated in Figure 5. A comparison between the simulation and experimental results is shown in Figure 5, where the effect of the fluid inlet temperature is investigated. There is a good agreement of the simulation results with the experimental data. It can be seen that the total amount of deposition increases with the inlet temperature and that fouling is at a low level in the inlet region and then increases significantly at some point down the tube. It should be emphasized here

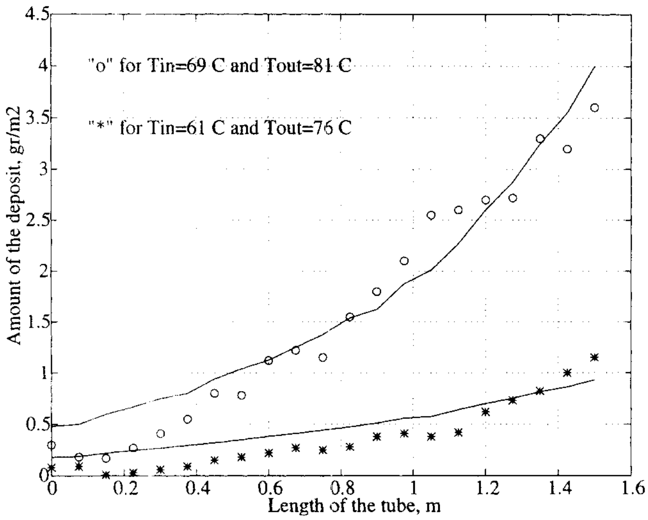

Figure 5. Comparison between simulation and experimental results.

that in the parameter estimation problem the two sets of experimental conditions (different inlet and outlet temperatures) are analyzed simultaneously.

The effect of Reynolds number on fouling and comparison with experimental results is shown in Figure 6. Again, the experimental results were taken from Belmar-Beiny et al. (1993). We observe that as the Reynolds number increases the total amount of deposit down the tube decreases. There is a quite good agreement with the experimental work although at low Reynolds number fouling is overestimated. The Reynolds number in our model was modified by changing the milk flow rate for constant diameter. The experimental conditions were: 1% whey protein, fluid inlet temperature 73°C and outlet 83°C, heating time 1 h.

Simulation results and discussion

The fouling behavior of four different heat-exchanger configurations was then investigated (see Table 3). The inlet native protein concentration in all cases is 3.8 kg/m^3. The key

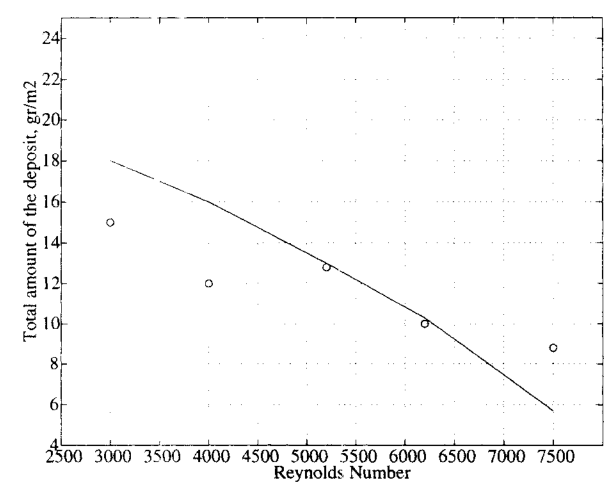

Figure 6. Effect of Reynolds number and comparison with experimental results.

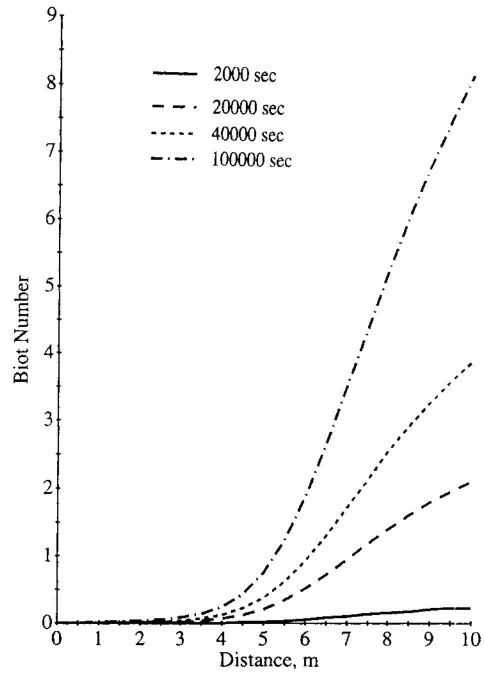

Figure 7. Biot number profile for $T_w = 374$ at different times.

role of some of the model's parameters is also illustrated. The main results are summarized as follows:

- Figure 7 depicts the profile of Biot number (fouling resistance) at different times for case 1 (constant wall temperature operation $T_w = 374$ K). The Biot number increases with respect to time and along the tube. This indicates that fouling is greatly affected by reactions. Since the bulk and interface temperature increase along the tube, this also increases the rate of the protein reactions and therefore the concentration of layer aggregated protein and finally the Biot number.
- The deposit thickness follows a similar pattern with the Biot number increasing its value along the tube (Figure 8). Here, again the first case of operation is studied. Similar profiles are obtained for the mass of the deposit as shown in the comparison with the experimental results (see Figure 5).
- As expected, the overall heat-transfer coefficient decreases with time (Figure 9). This refers to the 374 K uniform wall temperature. The overall heat-transfer coefficient at the end of the time horizon reaches the value of 1,500 W/m^2·K and the corresponding value under clean conditions is 3,100 W/m^2·K. Similarly, the milk outlet temperature reaches the value of 362 K (Figure 10). It should be noted here that the rate of fouling decreases with time following the decrease in milk outlet temperature. However, for the case where control action is applied (that is, increasing steam temperature) this may not be the case since more heat will be provided to the system in order to maintain milk outlet temperature close to its target value.
- Finally, the four cases of operation are compared in Figure 10. We observe that the constant wall temperature case (390 K) results in the most severe drift in milk outlet temperature. Countercurrent operation also causes a significant decrease in the heat-exchanger thermal performance. The final results are summarized in Table 5. We note that a heat exchanger operating at 374 K will suffer an 8 K drop outlet

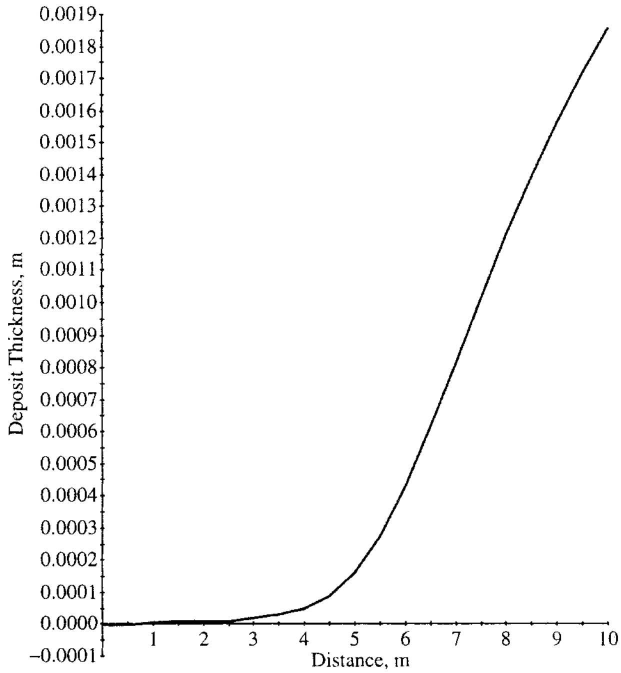

Figure 8. Deposit thickness profile for heating time 100,000 s.

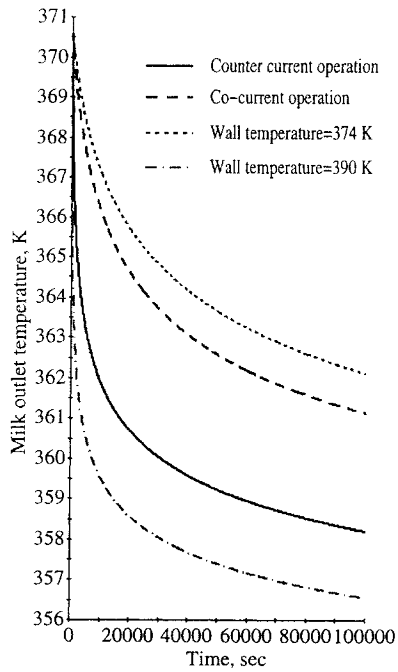

Figure 10. Effect of all cases of operation on milk outlet temperature.

temperature after 27.5 h, while the corresponding value for one at 390 K is just 1.4 h. Thus, although the higher temperature option has a lower capital cost, the downtime for cleaning will be significantly higher.

Sensitivity analysis

The mathematical model presented earlier includes a number of parameters such as the initial protein concentrations.

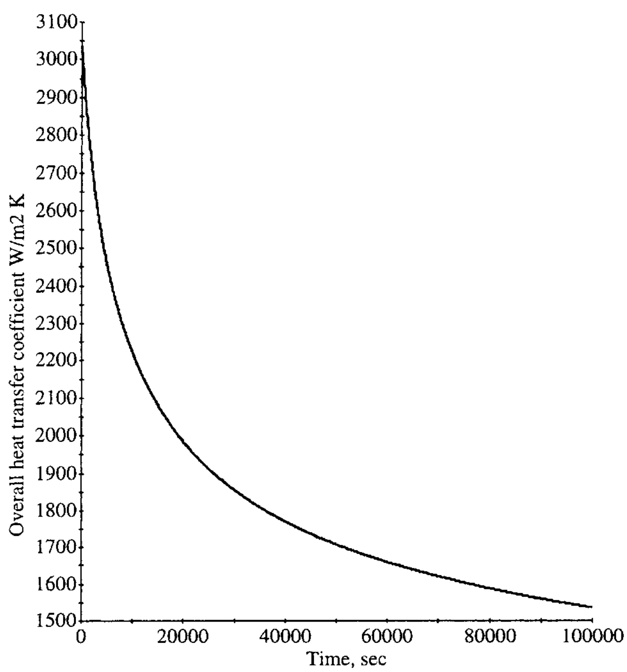

Figure 9. Overall heat-transfer coefficient.

The values of these parameters are uncertain due to variability in the milk quality. For example, there is a seasonal variation of the inlet native protein (Grandison, 1988). Here, we investigate the impact of these parameters on the milk outlet temperature and the results for the constant wall temperature case (374 K) are summarized as follows:

- Figure 11 depicts the effect of a 32% change in the initial native protein concentration on fouling. The total drift in the milk outlet temperature when the initial protein concentration is 2.5 kg/m^3 decreases by 30% compared to the nominal case where the concentration was 3.8 kg/m^3. Clearly, there is a significant effect of milk composition on fouling.
- In Figure 12, the Reynolds number is increased to the value of 14,000 (by increasing the milk flow rate) from 8,800 (nominal case). We observe that substantial mitigation of fouling is achieved (almost 60% reduction). This result provides some justification for the current industrial practice where milk is processed at the highest possible velocity. A similar effect of Reynolds number on fouling was also illustrated experimentally by Belmar-Beiny et al. (1993) and Toyoda and Fryer (1997).
- The effect of having a fraction of denaturated protein at the inlet of the heat exchangers is depicted in Figure 13. We observe that higher fouling exists compared to the nominal case where there is no denaturated protein. The existence of

Table 5. Effect of Fouling on Milk Outlet Temperature for Four Cases of Operation

Case of Oper.	Type of Exchanger	Drift in Milk Outlet Temp, K
1	Steam, $T_w = 374$ K	8.3
2	Steam, $T_w = 390$ K	13.9
3	Hot water, cocurrent flow	9.4
4	Hot water, countercurrent flow	12

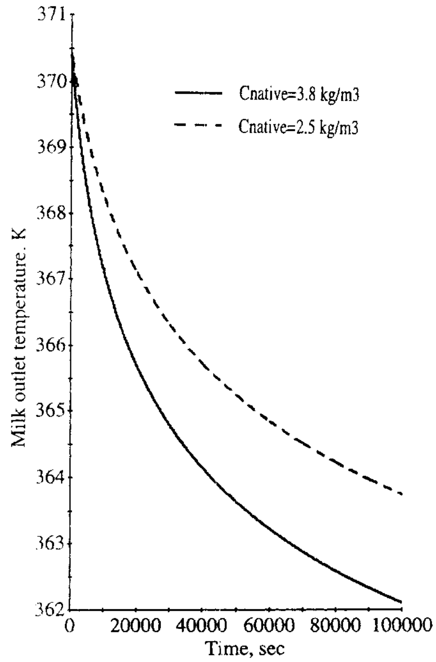

Figure 11. Native protein concentration effect on fouling.

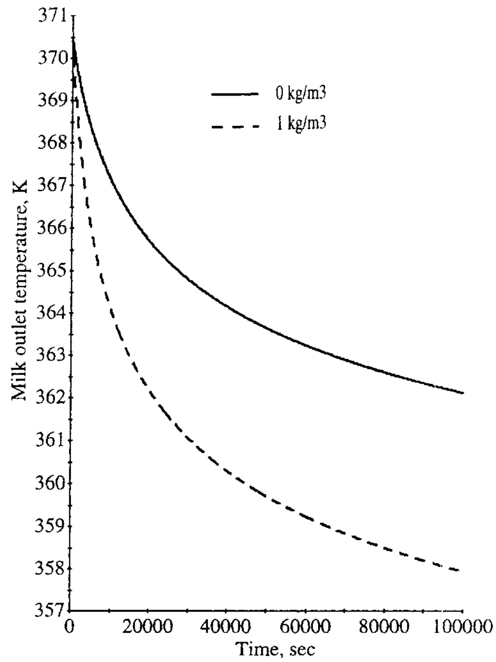

Figure 13. Effect of initial denaturated protein on fouling.

this protein at the inlet may arise from previous thermal milk treatment. Here it was assumed that the initial concentration of the denaturated protein was 1 kg/m^3.

The simulation results are intuitively correct and changes in important parameters lead to the expected conclusions. Therefore, the presented model describes all the important heat and mass transport phenomena occurring during fouling in a realistic way, while current industrial practice for milk fouling mitigation is qualitatively supported. It is worth noticing here that if a control action will be applied by increasing steam or hot water inlet temperature (in order to maintain milk outlet temperature close to its target value), fouling will become more severe. This is due to the increased wall temperature, which will give rise to faster reaction rates.

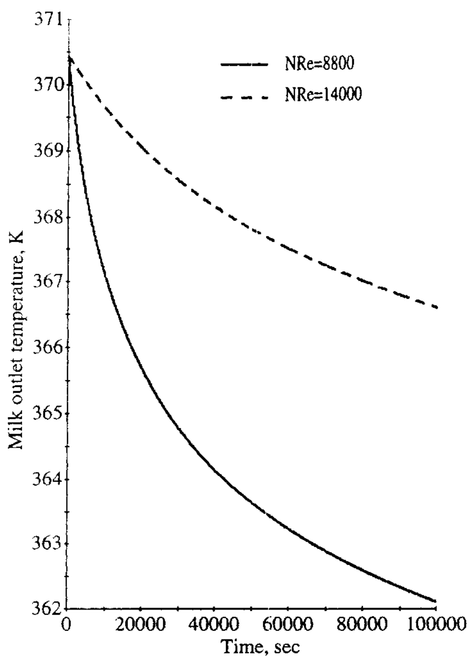

Figure 12. Effect of Reynolds number on fouling.

An important conclusion is that for a given thermal duty short exchangers appear to give the most severe drift in milk outlet temperature. This view supports the operating heuristic commonly employed in dairy plants that in order to minimize fouling, milk should be heated as gradually as possible.

In general, the mathematical models presented in this article are based on fundamental physical laws (under the specified assumptions) to capture and quantify the effect of milk fouling on the heat-exchanger performance. The results obtained, since they rely on physical based models, may be extrapolated to unexplored regions, or in other words to help in solving the scale-up problem which implies extrapolation. In this context the models presented here may also allow the design of optimal control strategies and/or operations to be studied.

Conclusions

We have developed a general mathematical model of single shell-and-tube heat exchangers under milk fouling. The model can be also used for heat exchangers which are subjected to fouling caused by chemical reaction(s). All transfer phenomena which take place during milk heat treatment were quantified in a formal way and a large number of variables were monitored to study the behavior and effect of fouling on the heat-exchanger performance. Despite its complexity, the model can be simulated successfully using currently available modeling tools such as gPROMS. Good agreement of the simulation results with experimental data has been achieved based on the solution of dynamic parameter estimation problem. Typical industrial operating techniques for fouling mitigations were verified. Examples have been presented to illustrate the behavior of fouling for four different configurations of tubular heat exchangers.

There exists a tradeoff between operating costs such as cleaning and capital costs. A larger heat-exchanger area will decrease the cleaning duties but will simultaneously increase capital costs. As mentioned by Fryer (1989), for any given thermal duty, an optimum heat-exchanger size exists that balances the reduced operating cost and fouling afforded by large heat exchangers against their increased capital cost. Furthermore, the switching time from heating to cleaning and the control policy (in order to maintain milk temperature close to its target value) must also be optimally selected. So far, no attempt has been made to optimize heat exchangers under fouling taking into account all the cost factors related to the milk heat treatment and using rigorous dynamic models. It is envisaged that the model presented here can provide the basis for such an exercise, and this is an avenue we are currently exploring (Georgiadis et al., 1998).

Notation

Area = cross-sectional area of the tube, m
C_N^* = layer native protein concentration, kg/m^3
C_D^* = bulk denaturated protein concentration, kg/m^3
C_A^* = bulk aggregated protein concentration, kg/m^3
C_p = milk specific heat capacity, J/kg·K
C_{pw} = heating medium specific heat capacity, J/(kg·K)
k_f = milk thermal conductivity, W/(m·K)
$\overline{\text{mass}}$ = average deposit mass, g/m^2
T_f^{in} = milk steady state inlet temperature, K
T_m^{out} = milk dynamic outlet temperature, K
T_s^{in} = heating medium steady state inlet temperature, K
T_s^{out} = heating medium steady state outlet temperature, K
u_z = milk velocity, m/s
δ = laminar layer
ϵ_{fic} = fictitious efficiency of the exchanger
μ = milk viscosity, kg/m·s
ρ = milk density, kg/m^3
ρ_w = heating medium density, kg/m^3

Acknowledgments

The authors thank Professor Costas Pantelides in the Centre for Process Systems Engineering at Imperial College for his helpful comments and suggestions. Financial support by EPSRC is also gratefully acknowledged.

Literature Cited

Barton, P. I., and C. C. Pantelides, "The Modeling of Combined Discrete/Continuous Processes," *AIChE J.*, **40**, 966 (1994).
Belmar-Beiny, M. T., S. M. Gotham, W. R. Paterson, and P. J. Fryer, "The Effect of Reynolds Number and Fluid Temperature in Whey Protein Fouling," *J. Soc. of Dairy Technol.*, **19**, 119 (1993).
Brodkey, R. S., and H. C. Hershey, *Transport Phenomena: A Unified Approach*, McGraw-Hill, Singapore (1988).
Danckwerts, P. V., "Continuous Flow Systems: Distribution of Residence Times," *Chem. Eng. Sci.*, **2**, 1 (1953).
De Jong, P., S. Bouman, and H. J. Van Der Linden, "Fouling of Heat Transfer Equipment in Relation to the Denaturation of β-lactoglobulin," *J. Soc. of Dairy Technol.*, **45**, 3 (1992).
Delplace, F., and J. C. Leuliet, "Modelling Fouling of a Plate Heat Exchanger with Different Flow Arrangement by Whey Protein Solutions," *Trans. I. Chem. E. Part C*, **73**, 112 (1995).
Delplace, F., J. C. Leuliet, and J. P. Tissier, "Fouling Experiments of Plate Heat Exchangers by Whey Protein Solutions," *Trans. I. Chem. E. Part C*, **72**, 163 (1994).
Fryer, P. J., "The Uses of Fouling Models in the Design of Food Process Plant," *J. Soc. of Dairy Technol.*, **42**, 23 (1989).
Fryer, P. J., and N. K. H. Slater, "A Direct Simulation Procedure for Chemical Reaction Fouling in Heat Exchangers," *Chem. Eng. J.*, **31**, 97 (1985).
Fryer, P. J., P. T. Robins, C. Green, P. J. R. Schreier, A. M. Pritchard, A. P. M. Hasting, D. G. Royston, and J. F. Richardson, "A Statistical Model for Fouling of a Plate Heat Exchanger by Whey Protein Solution at UHT Conditions," *Trans. I. Chem. E. Part C*, **74**, 189 (1996).
Georgiadis, M. C., G. E. Rotstein, and S. Macchietto, "Optimal Design and Operation of Heat Exchangers under Milk Fouling," in press (1998).
gPROMS Technical Document, "The gEST Parameter Estimation Tool," Imperial College of Science Technology and Medicine, London (1997).
Grandison, A. S., "UHT Processing of Milk: Seasonal Variation in Deposit Formation in Heat Exchangers," *J. Soc. of Dairy Technol.*, **41**, 43 (1988).
Lalande, M., F. Rene, and J. P. Tissier, "Fouling and Its Control in Heat Exchangers in the Dairy Industry," *Biofouling*, **1**, 233 (1989).
Lalande, M., J. P. Tissier, and G. Corrieu, "Fouling of Heat Transfer Surfaces Related to b-Lactoglobulin Denaturation During Heat Processing of Milk," *Biotechnol. Prog.*, **1**, 131 (1985).
LeClercq-Perlat, M. N., and M. Lalande, "A Review on the Modelling of the Removal of Porous Contaminant Deposited on Heat Transfer Surfaces," *Int. Chem. Eng.*, **31**, 74 (1991).
McKetta, J. J., *Chemical Engineering Design Encyclopedia*, Marcel Dekker, New York (1984).
Oh, M., and C. C. Pantelides, "A Modelling and Simulation Language for Combined Lumped and Distributed Parameter Systems," *Comp. Chem. Eng.*, **20**, 611 (1996).
Paterson, W. R., and P. J. Fryer, "A Reaction Engineering Approach to the Analysis of Fouling," *Chem. Eng. Sci.*, **43**, 1714 (1988).
Perry, R. H., and D. Green, *Perry's Chemical Engineering Handbook*, McGraw-Hill, New York (1984).
Sandu, C., "Physicomathematical Model for Milk Fouling in a Plate Heat Exchanger," PhD Thesis, Univ. of Wisconsin-Madison (1989).
Sandu, C., and D. Lund, "Fouling of Heat Transfer Equipment by Food Fluids: Computational Models," *AIChE Symp. Ser.*, **78**, 12 (1982).
Sandu, C., and D. Lund, "Fouling of Heat Exchangers: Optimum Design and Operation," *Fouling of Heat Exchanger Surfaces*, Engineering Foundation, New York (1983).
Sandu, C., and R. K. Singh, "Energy Increase in Operation and Cleaning Due to Heat-Exchanger Fouling in Milk Pasteurization," *Food Technol.*, **23**, 84 (1991).
Toyoda, I., and P. J. Fryer, "A Computational Model for Reaction and Mass Transfer in Fouling from Whey Protein Solutions," *Fouling Mitigation of Industrial Heat Exchange Equipment*, Begell House, New York (1997).

Appendix: Parameter Estimation

The model described by Eqs. 1 to 77 after the discretization over the two axial domains can be presented in a general form as follows:

$$f[x(t), \dot{x}(t), y(t), u(t), p, \theta] = 0 \tag{A1}$$

where

- $x(t)$ and $y(t)$ are the differential and algebraic equations in the model; $\dot{x}(t)$ are the time derivatives of $x(t)$ (that is, $\dot{x} \equiv dx/dt$).
- $u(t)$ and p are the time-varying and time-invariant control parameters respectively; these describe the experiment(s) being carried out.
- θ are the unknown parameters to be estimated.

For the model considered here,

- Concentrations, temperatures, and the Biot number are the differential variables and all the others are the algebraic variables.

- There are no time-varying and time invariant control parameters.
- Constant β and particle diameters are the unknown parameters to be estimated.

The initial conditions of the system are specified.

The parameter estimation problem makes use of experimental results gathered from a set of experiments. In general, we can have any number L of such experiments. Each experiment l ($l = 1 \ldots L$) is characterized by

- Its overall duration
- Its initial conditions
- Variation of the control variables
- Values of the time invariant parameters p.

Associated with each experiment l are also a set of data pairs collected during the experiment. These are of the form

$$(t_{lik}, \hat{z}_{lik}) \tag{A2}$$

where $\hat{z}_{lik}$ is the kth value measured for variable z_i during experiment l, and t_{lik} is the time at which this measurement was taken. In our problem, z_i is the deposit mass for which experimental data are available at time 1 h and for different positions along the tube. There are two sets of experiments l for the two different milk inlet and outlet temperatures. All these data were taken from Belmar-Beiny et al. (1993). Note also that, in the general case, the measurement instants do not need to be equispaced; nor, is it necessary for all measured variables to be recorded at the same time.

The parameter estimation problem attempts to determine values for the unknown parameters θ that minimize the deviation between model predictions and experimental data. More specifically, a least-square formulation is used here that seeks to determine the value of θ that minimizes the following objective function

$$\min_{\theta} \Phi = \sum_{l=1}^{L} W_l \sum_{i=1}^{I} w_i^2 \sum_{k=1}^{K} \left[z(t_{lik}) - \hat{z}_{lik} \right]^2 \tag{A3}$$

This is the weighted sum of the squares of the differences between the model predictions $z(t_{lik})$ and the experimentally measured values $(\hat{z}_{lik})$.

In the objective function above, the deviations corresponding to different variables i are scaled using coefficients w_i. This can be useful for the cases where some measurements are more reliable than others. In such cases higher values to w_i are assigned for the high priority measurements. Similarly, deviations arising from different experiments are weighted using W_l weighting factors.

For the problem considered here, we assume that both experiments were performed under approximately the same conditions, and, thus, we do not have any reason for trusting the one set of data experiment more than the other. Therefore, we can choose

$$W_1 = W_2 = 1.0 \tag{A4}$$

Similarly, all the variables weights w_i are also to one.

The parameter estimation problem described above with the objective function given by Eq. A3 together with the model Eqs. 1 to 77 is a dynamic optimization problem which is formulated and solved using the gEST tool. The last can be used to specify and perform parameter estimation calculations using processes defined in the gPROMS language (gPROMS Technical Document, 1997).

Manuscript received May 27, 1997, and revision received Jan. 20, 1998.